Published in final edited form as:
Oncogene. 2013 June 27; 32(26): 3165–3174. doi:10.1038/onc.2012.322.

p53 isoform profiling in glioblastoma and injured brain

Rie Takahashi, B.S.[1,2], **Caterina Giannini, M.D., Ph.D.**[3,6], **Jann N. Sarkaria, M.D.**[4], **Mark Schroeder**[4], **Joseph Rogers, Ph.D.**[5], **Diego Mastroeni, B.S.**[5], and **Heidi Scrable, Ph.D.**[2,6,7,*]

[1]Mayo Clinic Medical Scientist Training Program, Rochester, MN 55905

[2]Mayo Clinic Department of Biochemistry and Molecular Biology, Rochester, MN 55905

[3]Mayo Clinic Division of Anatomic Pathology, Rochester, MN 55905

[4]Mayo Clinic Department of Radiation Oncology, Rochester, MN 55905

[5]Banner Sun Health Research Institute, Sun City, Arizona 85351

[6]Mayo Clinic Department of Laboratory Medicine and Pathology, Rochester, MN 55905

[7]Mayo Clinic Robert and Arlene Kogod Center on Aging, Rochester, MN 55905

Abstract

The tumor suppressor p53 has been found to be the most commonly mutated gene in human cancers; however, the frequency of *p53* mutations varies from 10–70% across different cancer types. This variability can partly be explained by inactivating mechanisms aside from direct genomic polymorphisms. The p53 gene encodes 12 isoforms, which have been shown to modulate full-length p53 activity in cancer. In this study, we characterized p53 isoform expression patterns in glioblastoma, gliosis, non-tumor brain, and neural progenitor cells by SDS-PAGE, immunoblot, mass spectrometry, and RT-PCR.

At the protein level, we found that the most consistently expressed isoform in glioblastoma, Δ40p53, was uniquely expressed in regenerative processes, such as those involving neural progenitor cells and gliosis compared to tumor samples. Isoform profiling of glioblastoma tissues revealed the presence of both Δ40p53 and full-length p53, neither of which were detected in non-tumor cerebral cortex. Upon xenograft propagation of tumors, p53 levels increased. The variability of overall p53 expression and relative levels of isoforms suggest fluctuations in subpopulations of cells with greater or lesser capacity for proliferation, which can change as the tumor evolves under different growth conditions.

Keywords

gliosis; regeneration; astrocytoma

Introduction

The tumor suppressor p53 has been found to be the most commonly mutated gene in human cancers (1–5). However, the frequency of *p53* mutations in each individual cancer type

*Corresponding Author (Scrable.Heidi@mayo.edu).
Addresses
Mayo Clinic, 200 First Street S.W., Rochester, MN, 55905
Banner Sun Health Research Institute, 10515 West Santa Fe Drive, Sun City, AZ 85351

Conflict of Interest
Authors have no conflicts of interest to claim with respect to this research.

varies from 10 to 70% (6–9). These data suggest that mechanisms aside from direct p53 gene mutation may be important in cancer development, and specifically in glioblastoma, *p53* mutations have not been identified as a necessary step in tumor progression (6, 10).

The *p53* gene has been documented to encode a family of 12 isoforms, which have been found in both cancer (11–15) and normal development (16). A specific function for each isoform has yet to be defined, though some p53 isoforms have been shown to alter the function of the parent p53 (11–14, 17, 18). Δ40p53 (also known as ΔNp53, p44, or p53/47) was first identified in the mouse as a naturally occurring isoform present in Friend virus-induced tumors lacking full-length p53 [19,20]. Subsequent studies have focused on investigating endogenous p53 isoform expression in human cancers (11, 13, 14, 19). The complexity of determining the frequency and mode of non-genomic p53 inactivation in cancers can be partly attributed to the function of the numerous p53 isoforms (1, 20).

p53 mutations and protein levels have been extensively characterized in tumors primarily by sequencing and immunohistochemistry (1, 2); however, these methods alone are insufficient in distinguishing specific isoforms due to the complex regulation of p53 at the transcriptional, translational, and intermolecular level (20, 21). This is particularly true for Δ40p53, which can only be reliably detected using protein-based methods. Although most p53 isoforms arise by alternative splicing or alternate promoter usage (20), Δ40p53 is generated primarily by a mechanism involving alternative translation initiation of an mRNA shared with full-length p53. Utilization of a start site in exon 2 initiates at amino acid 1 and generates p53, while utilization of a start site in exon 4 initiates at amino acid 41 and produces Δ40p53 (22–25). Δ40p53 can also be expressed by alternative splicing of intron 2 in some cell types (12, 17, 18, 26), but such a mechanism contributes only a minor portion of total Δ40p53 levels (17, 27).

Given that p53 executes its primary function as a transcription factor, which is a tetramer of p53 monomers that require both N- and C-terminal domains for full activity, isoforms that differ in their domain structure could significantly alter function, even in the absence of *p53* sequence changes. We characterized p53 isoform expression patterns in glioblastoma, gliosis, non-tumor brain, and neural progenitor cells using a combination of methods including (but not limited to) SDS-PAGE, immunoblot, and mass spectrometry. Such an approach allowed us to examine differences in endogenous p53 isoform protein patterns across tumor and non-tumor brain specimens.

Results

Δ40p53 is a major isoform in GBM

We initially examined 17 glioblastoma xenograft tissues (GBM XT) for p53 isoform expression by western blot analysis using CM1, a polyclonal antibody against p53 (Fig. 1A). The tumors were derived from 12 male, 3 female, and 2 unidentified patients ranging in age from 41 to 82 years (mean age 62), and were located either in the parietal, frontal, or temporal cortex, or in the cerebellum (Table I). We detected a total of three immunoreactive bands between the 37 and 50kD markers in this initial panel of tumors. In addition to p53 at approximately 50kD, these bands could represent any one of four isoforms that migrate with apparent MWs within this range: Δ40p53 (48kD); p53β (46kD); p53γ (46kD), and Δp53 (44kD). Although very similar in MW, these isoforms lack specific regions of the full-length protein, as diagrammed in Fig. 1B, and are easily distinguished from one another using epitope-specific antibodies. Epitopes recognized by the various antibodies used in this study are indicated at the top of the diagram in Fig. 1B. Δ40p53 is missing the N-terminal 40 amino acids (Fig. 1B, region indicated as "TFD-1"), and can be differentiated from the other three using monoclonal antibodies DO1, DO7, DO13, and BP53-12, which map in this

region. p53β and p53γ have alternate C-terminal amino acids and lose the epitope detected by pAb421. Δp53 is missing amino acids in the central region of the protein, but retains both the N-terminal epitope missing in Δ40p53 and the C-terminal epitope missing in p53β and p53γ. To identify the isoforms prevalent in the tumors, we used the N-terminal monoclonal antibody DO1 and the C-terminal monoclonal antibody pAb421 on the same panel of GBM XT (Fig. 1A). Using DO1, we found a band at approximately 50kD in 16 of 17 tumors (Fig. 1A, DO1) and a band slightly above 37kD in less than half of the samples (most visible in GBM XT 28 and 36, Fig. 1A, DO1). Using pAb421 (Fig. 1A, pAb421), we saw the appearance of a band not found in DO1 at approximately 45kD in 16 of 17 samples. This 45kD band detected by pAb421 did not overlap with the band migrating slightly above 37kD that was detected by DO1 (Fig. 1A, DO1/pAb421 overlay). We noted a difference in p53 detection by pAb421 compared to CM1 and attributed this difference to the sensitivity of pAb421 to post-translational modifications. Based on the known p53 isoforms that migrate at approximately 45kD, the isoform that would be detected by pAb421 but not DO1 is Δ40p53 (Fig. 1B). We tentatively identified this 45kD band as Δ40p53.

To verify the identity of p53 isoforms in GBM, we first used RT-PCR and primers that would amplify p53 and several different isoforms (Fig. S1). We used standard RT-PCR conditions to amplify the unique intron 2 sequence found in Δ40p53 generated by alternative splicing (12), and successfully amplified the predicted 360bp amplicon (Fig. S2A). However, sequencing results did not match the unique Δ40p53 intron 2 sequence. This suggested that alternative splicing was not the major mechanism involved in Δ40p53 production. Next, we used both single and nested PCR protocols designed to amplify p53β and p53γ (28). Using a single PCR reaction with p53β primers, we were able to detect products at the predicted size for p53β in GBM XT 10, 12, 16, and 22 at low levels. We did not find amplicons corresponding to p53γ at the predicted 1kb size (Fig. S2B). Using nested PCR (see Supplemental Fig. 1A figure legend for details), however, we did not detect amplicons corresponding to either p53β or p53γ transcripts at the predicted 1kb size, and we verified these results by sequencing (Fig. S2C-E). The low transcript levels of p53β seen with single PCR analysis corresponded to faint bands migrating above the Δ40p53 band on western blots that were detected by DO1 but not pAb421 (Fig. 1A, best visualized in GBM XT16).

To continue with our analysis, we immunoprecipitated p53 proteins from GBM XT 43 (which expressed proteins at both 50 and 45kD, as shown in Fig. 1A) using DO1 or pAb421 monoclonal antibodies, the latter of which would not pull-down β/γ isoforms. The immunoprecipitated lysates were run on SDS-PAGE and silver stained (Fig. 2A) and major bands were submitted for mass spectrometric analysis. We identified the band co-migrating with the 50kD marker (Band 2) as full-length p53 based on the recovered peptide sequences, which are indicated in red in Fig. 2A. We identified the faster migrating band (Band 3) precipitated by the C-terminal pAb421 antibody as Δ40p53 based on apparent MW and the peptides recovered in the band, which span both the region deleted in Δp53 (**vcacpgr** and **alpnntssspqpk**) and the C-terminal domain missing in p53β and p53γ (**elnealelk**). No p53 peptides were recovered from bands 1 or 4.

To compensate for the failure of mass spectrometry to detect any N-terminal peptides in bands 2 and 3, which would have allowed unambiguous identification of p53 or Δ40p53, we utilized a panel of monoclonal antibodies against epitopes in the N-terminal domain of p53 with isogenic cell lines that express either p53 and Δ40p53 or only Δ40p53. We compared immunoreactive bands in lysates from HCT116 colorectal cancer cells, which have a wildtype *p53* (HCT116+/+), and from the HCT116 p53−/− isogenic subline (Fig. 2B). The HCT116−/− subline was derived by targeting a neomycin-resistance gene into the first codon of the *p53* gene within exon 2 (29). The recombinant allele can no longer make full-

length p53, p53β or p53γ, which initiate in exon 2. However, it can and does produce Δ40p53 from the intact start codon in exon 4 utilized by endogenous Δ40p53. Thus, HCT116−/− cells can be used as a control in which the Δ40p53 isoform is expressed in the absence of full-length p53. As shown in Fig. 2B, the polyclonal antibody CM1 detects a pair of bands in extracts of HCT116+/+ cells, but only the lower of these two bands in HCT116−/− cells. N-terminal antibodies (DO1, DO7, and BP53-12) react with the upper band, which migrates at approximately 50kD, and a lower band migrating at approximately 44kD, but not the band migrating at approximately 48kD (Fig. 2B). Based on the known genotype of HCT116+/+ and −/− cells, the 50kD and 48kD bands represent p53 and Δ40p53, respectively. Comparing these positively identified bands with bands detected in extracts from GBMs, we can unambiguously identify the single isoform present in GBM XT 22 as p53 (Fig. 2B, CM1, arrow) and the single isoform present in GBM XT 12 as Δ40p53 (Fig. 2B, CM1, arrowhead). Thus, using the combination of mass spectrometry data and alignment with HCT cell lines expressing either p53 and Δ40p53 or Δ40p53 alone (Figure 2A and B), we have been able to assign p53 and Δ40p53 to specific bands detected by antibody CM1 in GBM. We find that Δ40p53 is highly and consistently expressed in GBM. Full-length p53, as detected by the N-terminal-specific monoclonal antibody DO1 (Fig. 1B), is increased relative to Δ40p53 in some of the samples derived from tumors with an identified DNA binding domain mutation (GBM XT 6, 12, 22, 28, 36, and 43), as detailed in Table I. We detected additional higher molecular weight bands with CM1 in the GBM XT panel, which are marked with one, two, or three asterisks on the full-sized western blots presented in Fig. S2. The bands marked with one or two asterisks were also found in cells lacking p53 (Fig. S3A), indicating that they do not represent any p53 isoform. The band marked with three asterisks was only present in cells with p53, but it was not recognized by antibodies against SUMO, Hsp70, p63, or p73, (Fig. S3B) and its identity remains unknown. We also detected one prominent lower MW band with CM1 in the GBM XT panel. This band, which migrated just above the 37kD marker, was detected in non-tumorous samples, gliosis (GLS 8) and cerebral cortex (CTX 9), as well p53-null cells (p53−/− NSC, H1299, LNZ308) (Fig. S4), indicating that it, too, does not represent a form of p53.

Next, we used unambiguously identified isoforms in GBM XT 22 and GBM XT 12 (Fig. 2B) as reference standards to aid in the assignment of co-migrating bands in samples of glioblastoma patient tissue (GBM PT), cerebral cortex (CTX), and gliosis (GLS) (Fig. 2C-E). First, we compared p53 isoform expression in GBM xenografts to that in primary tumors from patients diagnosed with Grade IV astrocytoma (glioblastoma multiforme) according to the WHO Classification of Central Nervous System Tumors (30). Tumors surgically removed from frontal, temporal, parietal or parieto-occipital brain regions were obtained from 7 male and 3 female patients aged 23 to 78 years (average 56 years) (Table II). Compared to p53 peptides detected by CM1 in xenograft samples (Fig. 1A), smaller molecular weight p53 isoforms (<50kD) were detected at lower levels in primary tumor samples (Fig. 2C). There was a band corresponding to Δ40p53 in over half of the samples, most visibly in sample 5. Full-length p53 was detected at approximately 50kD, most prominently seen in samples 8 and 10. We could not detect p53 isoforms below the 37kD marker. In summary, of the p53 species detected by CM1, one of the most consistently expressed isoform in both GBM xenograft and patient material is Δ40p53. Full-length p53 is found less frequently, but can be detected at high levels in some tumors. Overall, p53 isoforms were detected at lower levels in patient-derived compared to xenograft-derived GBM.

Full-length p53 is associated with the tumor component of GBM PT

To resolve the discrepancy in the levels of p53 isoforms detected in patient-derived (Fig. 2C) and xenograft-derived (Fig. 1A) GBM, we compared p53 expression in primary tumors

and serial passages of the same tumor engrafted into nude mice. Protein lysates were extracted from tumors at passage 1, 2, and 4 or 5 and compared to primary tumors by SDS-PAGE and western blot analysis using DO1 and CM1 (Fig 3). GBM 43 served as a control for p53 (arrow) and Δ40p53 (arrowhead). We found that Δ40p53 was expressed in 4 out of 5 primary GBMs and in all xenograft samples (48kD band detected by CM1 and not DO1). We could not detect p53 in any of the primary GBM samples; however, p53 was apparent in all passages of 4 out of 5 xenografts. Only GBM 121 did not express p53 in primary or xenograft conditions and was similar to GBM 12 (Fig. 1A) in that only Δ40p53 could be detected. We noted that GBM 132 had increased levels of p53, which mimicked the levels seen in GBM xenografts with p53 DNA binding domain mutations (Fig. 1 single asterisk and Table I). To determine if p53 expression was a transient or long-term effect, we also examined xenografts from passages 30, 35, and 46 and found that p53 continued to be expressed in later passages (Fig. S5). We confirmed that the increase in p53 upon serial passage was not due to contamination by surrounding host mouse tissue by using DO1, which detects an epitope in human p53 not present in mouse p53 (Fig. 1B). The p53 band did not disappear with DO1 (Fig. 3, DO1 panel), indicating that the 50kD band detected by CM1 was in fact human p53. In summary, removal and growth of patient tumor sample in the environment of the nude mouse revealed full-length p53. This change in p53 expression occurred within the first passage in nude mice concurrent with the expansion of the tumor component of the resected material and was retained even in late passage serial xenografts.

Injury induces Δ40p53 in brain

To determine if these patterns of p53 isoform expression were unique to tumors, we examined p53 isoform expression in 9 cerebral cortex samples from autopsy and 10 temporal lobe seizure resections classified as gliosis (reactive astrocytosis) (Fig. 2D and E). Cerebral cortex specimens were collected from patients (5 female, 4 male) whose cause of death was unrelated to brain pathology. In contrast to glioblastoma specimens, gliosis and cerebral cortex tissues exhibited a uniform p53 expression pattern across individual samples. Normal cortex was devoid of p53 expression (Fig. 2D). Gliotic samples, on the other hand, consistently expressed Δ40p53 (Fig. 2E). There was a complete and striking absence of full-length p53 in both gliosis and normal cortex compared to xenograft- and patient-derived GBM (Fig. 1A and 2C). Consistent Δ40p53 expression in the absence of p53, therefore, is the distinguishing feature of tumorous vs. non-tumorous brain.

Δ40p53 is a constituent of subventricular zone (SVZ) progenitor cells

GBMs have been proposed to arise from the common glial/neuronal precursor cells (NSCs) present in neurogenic regions of the adult brain (31–34). This theory is supported by behavioral and molecular characteristics shared by both cancer and progenitor cells, such as multipotency, proliferative capacity, signaling pathways, and protein expression (35–38). To determine if the expression of p53 isoforms in glioblastoma might reflect that found in normal adult human neural progenitor cells, we cultured cells derived from the subventricular zone (SVZ) of elderly human subjects obtained by rapid autopsy protocol (39). Cells were grown either in the presence of serum or of epidermal and fibroblast growth factors (EGF and FGF, respectively). When cells were propagated with EGF and FGF, >90% of the population of cells created neurospheres (NS), which did not adhere to the surface of the culture plate (Fig. 4A, top panel). On the other hand, when we replaced the growth factors with serum, cells grew as an adherent monolayer (ADH) with occasional, phase-bright foci that also adhered to the surface of the culture plate (Fig. 4A, bottom panel). Within this adherent culture, we visualized a heterogeneous population of cells, including those that resembled astrocytes (large cytoplasm with ruffled border) and others that resembled neurons, which had processes that were greater than 4 times the diameter of the cell body (Fig. 4, arrowheads). Similar cells were observed in the NS cultures, but were

infrequent and comprised only a small percentage of the total population. Our characterization of the adult human SVZ cells was consistent with the results of a previous study of similar cultures from human rapid autopsies (39).

Both adherent and non-adherent cultures of adult human SVZ cells expressed Δ40p53, but not full-length p53, in contrast to GBM, which expressed both and normal cortex that expressed neither (Fig. 4B). There was also more Δ40p53 in NS cultures and tumor cells compared to levels seen in ADH cultures, suggesting that actively proliferating cells may express more of this isoform. This is consistent with our previous observation that Δ40p53 is an embryonic isoform of p53 that is associated with proliferating populations of stem cells (16).

As the pool of NSCs is known to decrease with age (40), we used the model system of adult neurogenesis in the mouse to determine if the level of Δ40p53 also decreased in aging neural progenitor cell populations. We harvested neural progenitor cells from the subventricular zone (SVZ) of embryonic day 14 (E14), 2.5 month-old (2.5mo), and 14 month-old (14mo) mouse brain, as previously described (40), and compared the expression of p53 isoforms by western blot. As shown in Fig. 4C, we observed a decreasing trend in Δ40p53 expression with SVZ cells derived from older mice. Analysis of variation (ANOVA) did not show a statistically significant difference among the groups; however, we have consistently observed a decline in Δ40p53 levels within the aging brain. The low level of Δ40p53 in multipotent mouse neural progenitors specifically derived from older mice closely resembled the level of Δ40p53 in SVZ cells derived from elderly humans (Fig. 4B). Pluripotent embryonic stem cells (ESCs), on the other hand, with their prominent expression of both Δ40p53 and full-length p53 (Fig. 4C), more closely resembled the p53 isoform expression pattern seen in human GBM. We confirmed the identity of Δ40p53 using CM1 and an N-terminal monoclonal antibody against murine p53 (1C12), which reacted with p53 but not Δ40p53 in mouse cells (Fig. S6).

To determine if the loss of Δ40p53 expression with age might reflect the decreasing ability of aging NSCs to remain multipotent, we compared the expression of Δ40p53 in populations of murine SVZ cell cultures forced to undergo the transition from non-adherent (NS) to adherent monolayer (ADH) growth and then induced to differentiate into neuronal and glial progeny. Sequential removal of EGF and FGF resulted in a loss of Δ40p53 expression between days 0 and 4 in vitro, followed by an increase in Δ40p53 expression over the course of the next three days in the presence of serum (Fig. 5A-B).

At day 7 in vitro, cells were harvested and analyzed for the presence of differentiated progeny by immunocytochemistry (ICC) using antibodies against nestin, glial fibrillary acidic protein (GFAP), O_4, and β-tubulin. Representative images of murine and cultured human adult SVZ cells analyzed by ICC with these antibodies are presented in Fig. 5C. NSCs are nestin and GFAP double positive cells (nestin+GFAP+) (41–47) that have the potential to differentiate into an astrocyte (GFAP single positive), oligodendrocyte (O_4 single positive), or a neuron (β-tubulin single positive) (48–51). Based on the staining pattern of these differentiation markers, we concluded that the differentiation state of mouse embryonic NSCs at day 7 after growth factor withdrawal was comparable to adult human SVZ progenitor cells that had been grown in serum post-mortem. More specifically, the majority of mouse and adult human cells were either NSCs or astrocytes (Table III). Neurons were not detected in either cell population, and oligodendrocytes were only found in the human NSC population. A detailed description of each immunophenotype is given in the supplementary text accompanying Fig. S7. We concluded that the differentiation state (based on these markers) and levels of Δ40p53 seen in mouse SVZ cells resembled those seen in adult human-derived cells.

Again, the most remarkable difference between SVZ progenitor cells and glioblastoma cells was the complete absence of full-length p53. This pattern correlated with the appearance of differentiated cells identified by ICC with antibodies specific for immature and mature neuronal and non-neuronal derivatives of SVZ cultures.

Discussion

Using a set of previously characterized antibodies against p53 and mass spectrometry, we performed a comprehensive analysis of the isoform profiles in GBM, gliosis, non-tumor cortex, and neural progenitor cells. Several important findings emerged, which, against a background of previously described isoform profiles in human and mouse embryonic stem cells (16), poses the question of how and why certain p53 isoforms are preferentially expressed in certain contexts and what effects the isoforms may have on tumor development and response to therapy.

The distinguishing feature of GBM is the presence of both Δ40p53 and full-length p53, a profile also seen in pluripotent (embryonic) stem cells. Changes in the relative levels of these two p53 isoforms in ESCs can switch cells from the highly proliferative, pluripotent state of the undifferentiated ESC to that of a differentiated somatic cell with limited proliferative capacity and potency (16). The observation that the isoform profile of GBM xenografts resembles that of highly proliferative, undifferentiated stem cells may be a clue to the state of GBM cells relative to other cancer cells that may not express Δ40p53. In contrast, both adult SVZ progenitor cells and gliotic brain tissue undergo proliferation at much lower rates, and in response to injury, share a p53 isoform profile characterized by the expression of Δ40p53 in the absence of full-length p53. Furthermore, differentiated SVZ progenitor cells and tissue from normal brain express low to undetectable levels of Δ40p53 and no p53. In conclusion, the neural progenitor marker, Δ40p53, is increased in the astrocytic reaction to injury and in GBM, both of which have the capacity to proliferate (52, 53), but not in cerebral cortex that is primarily composed of terminally differentiated cells or in the differentiated progeny of SVZ progenitors.

A question that remains to be answered is how p53 isoforms, such as Δ40p53, function in the presence of mutant p53. A mutation in p53 would affect all isoforms containing the mutant domain. In the case of a heterozygous mutation, however, mutant and normal isoforms could interact, leading to situations in which a normal version of Δ40p53 could interact with a mutant form of p53 and rescue function. For example, a mutant p53 that is defective in DNA binding could pair together with a wildtype Δ40p53 competent for DNA binding, which could result in a heterotetrameric transcription factor. In the same heterozygous context, however, a mutant Δ40p53 isoform could have a dominant-negative effect on the wildtype p53 protein, similar to the dominant-negative effect of mutant p53 proteins on wildtype protein function (54–56). This could account for some of the variability seen in response to cancer treatment, as well as the mixed success of targeted p53 therapies.

Even in the absence of DNA sequence alterations, however, heterotetramers comprising p53 and Δ40p53 monomers could exhibit decreased or increased p53 tumor suppressor activity depending on how specific p53 targets are affected by the loss of one or more transactivation domains. Furthermore, because the Mdm2 binding domain is localized to the transactivation domain, heterotetramers with Δ40p53 could also reduce Mdm2 binding and increase the effective half-life of the transcription factor (23). This can explain the increased levels of p53 targets such as p21 in SVZ progenitor cells from mice with an increased dose of Δ40p53 (40). It is also possible that increased Δ40p53 in tumors could meet a compensatory increase in Mdm2 levels (though we did not observe increased Mdm2 expression in GBM xenografts, Fig. S8).

Deciphering the ultimate effects of increased p53 isoform expression in tumor development remains open for further study and is particularly warranted due to the increased levels of p53 seen in malignant cancers and pre-cancerous lesions even in the absence of mutations in the *p53* gene. One of the goals is to understand how the specific expression patterns of p53 isoforms in cancer compare to their expression in non-cancerous tissue that can undergo only limited proliferation. Insight into such endogenous isoform levels could provide novel approaches to controlling tumor growth through the orchestrator of cell fate, that is p53.

Materials and Methods

Mass spectrometry

Protein lysates were prepared from GBM XT 43 tumor tissue and immunoprecipitated using p53 antibodies, DO1 (Santa Cruz Biotechnology, Inc., Santa Cruz) and pAb421 (Calbiochem/EMD Chemicals, Gibbstown), as previously described (57). Immunoprecipitate were denatured and electrophoresed on a 10% Tris-HCl gel and silver stained according to manufacturer's protocol (Biorad, Hercules). Bands were excised from the gel and submitted for mass spectrometry analysis.

Western blot analysis

Protein lysates were prepared from frozen tissue samples and analyzed for p53 isoform expression by western blot (16). Protein concentration was determined using a BCA assay according to manufacturer's protocol (Biorad, Hercules). Nitrocellulose membranes were incubated overnight at 4°C with gentle shaking in primary antibodies at a 1:1000 dilution in either 1xTBST or blocking buffer (5% milk or BSA) as indicated. Antibody sources include the following: DO1 in 1xTBST (Santa Cruz Technologies, Inc., Santa Cruz), pAb421 in 1xTBST (Calbiochem/EMD Chemicals, Gibbstown), phospho-p53 (ser15P) in 5% BSA (Cell Signaling, Danvers), and CM1 in 5% milk (Vector Labs, Burlingame), SUMO-1 (Cell Signaling, Danvers), Hsp70 (Cell Signaling, Danvers), p63 (Cell Signaling, Danvers), p73 [5B1288] (Abcam, Cambridge), GAPDH (Ambion, Foster City) and actin (MPBio Biomedicals, Solon).

Patient, xenograft, and mouse samples

Frozen patient tissues were obtained from the Mayo Clinic Brain SPORE and Biospecimens Committee according to Institutional Review Board standards. Primary human glioblastoma multiforme xenografts were derived from human tissue as previously described(58). All tissues were frozen and maintained at −80°C until use. p53-null NSCs were derived from the SVZ of mice (Taconic Farms Inc., Hudson) and p53-competent ESCs were harvested from CD1 mice (Harlan Laboratories, Indianapolis) as previously described(16). H1299 and LNZ308 are human cancer cell lines (lung carcinoma and glioblastoma, respectively) that are p53-null(10, 59, 60). Mouse NSCs were maintained as spheres in the presence of EGF (20ng/mL) and FGF (20ng/mL) (Invitrogen, Carlsbad) in ultra-low attachment tissue culture plates (Corning, Lowell)(40). NSCs were plated on a poly-L-ornithine (PLO) treated surface in the absence of EGF on day 0, and the remaining FGF was replaced by 2% fetal bovine serum in DMEM (Gibco, Carlsbad) on day 3 before harvesting samples the following day(61). Adult human NSCs were cultured as either neurospheres (NS) in the absence of serum with growth factors, EGF (20ng/mL) and FGF (10ng/mL) (Peprotech, Rocky Hill) or as an adherent monolayer (ADH) with serum as previously described (39).

Immunofluorescence

Embryonic mouse and adult human NSCs were plated on PLO-treated and poly-L-lysine (PLL)-treated chamber slides (LabTek/Thermo Scientific, Rochester), respectively. Cells

were cultured in the conditions described above. Cells were fixed using 4% paraformaldehyde for 10 minutes and permeabilized with 0.1% Triton-X prior to staining with primary antibodies(40). The following antibodies and dilutions were used: mouse nestin (Chemicon, Billerica) at 1:50, human nestin (Millipore, Billerica) at 1:200, glial fibrillary acidic protein (GFAP) (DAKO, Carpinteria) at 1:500, β-tubulin (Sigma, St. Louis) at 1:400, and O_4 (Millipore, Billerica) at 1:50. Images of slides were captured with a 100x objective lens using an Axiophot fluorescence microscope and analyzed using Axiovision 4.8 software (Zeiss, Thornwood).

Supplementary Material

Refer to Web version on PubMed Central for supplementary material.

Acknowledgments

Funding

We would like to thank our Mayo Clinic colleagues for their contributions, in particular, Dr. Robert Jenkins for seminal discussions on the etiology of GBM and xenograft biology; Alissa Caron for preparing GBM patient tumor specimens; Dr. John Black for cerebral cortex samples; Guido Gonzalez for obtaining LNZ308 cells; and Benjamin Madden and the Mayo Clinic Protein Chemistry and Proteomics Shared Resource core for mass spectrometry analysis. We are grateful to past and current members of the Scrable lab for their enduring enthusiasm and abilities, in particular Dr. Erica Ungewitter for her invaluable help with p53 antibodies and the work she did as a graduate student that laid the foundation for subsequent studies on p53 in embryonic stem cells, and Dr. Silvia Medrano, for passing on her expertise with mouse NSC culture and the role of p53 in adult stem cells. This work was supported by PHS award R01AG026094 and a Senior Scholar in Aging award from the Ellison Medical Research Foundation to H.S. Additional support came from an NCI Cancer Center support grant to the Mayo Clinic Cancer Center, the Robert and Arlene Kogod Center on Aging at Mayo Clinic, the Mayo Brain Tumors SPORE, and the Mayo Clinic Medical Scientist Training Program (R.T.).

References

1. Machado-Silva A, Perrier S, Bourdon JC. p53 family members in cancer diagnosis and treatment. Semin Cancer Biol. 2010 Feb; 20(1):57–62. [PubMed: 20206267]
2. Robles AI, Harris CC. Clinical outcomes and correlates of TP53 mutations and cancer. Cold Spring Harb Perspect Biol. 2010 Mar.2(3):a001016. [PubMed: 20300207]
3. Hollstein M, Sidransky D, Vogelstein B, Harris CC. p53 mutations in human cancers. Science. 1991 Jul 5; 253(5015):49–53. [PubMed: 1905840]
4. Levine AJ, Momand J, Finlay CA. The p53 tumour suppressor gene. Nature. 1991 Jun 6; 351(6326): 453–456. [PubMed: 2046748]
5. Petitjean A, Mathe E, Kato S, Ishioka C, Tavtigian SV, Hainaut P, et al. Impact of mutant p53 functional properties on TP53 mutation patterns and tumor phenotype: lessons from recent developments in the IARC TP53 database. Hum Mutat. 2007 Jun; 28(6):622–629. [PubMed: 17311302]
6. Comprehensive genomic characterization defines human glioblastoma genes and core pathways. Nature. 2008 Oct 23; 455(7216):1061–1068. [PubMed: 18772890]
7. Butler T, Gribben JG. Biologic and clinical significance of molecular profiling in Chronic Lymphocytic Leukemia. Blood Rev. 2010 May; 24(3):135–141. [PubMed: 20398985]
8. Li W, Sanki A, Karim RZ, Thompson JF, Soon Lee C, Zhuang L, et al. The role of cell cycle regulatory proteins in the pathogenesis of melanoma. Pathology. 2006 Aug; 38(4):287–301. [PubMed: 16916716]
9. Soussi T. The TP53 web site. Paris. 2010 [updated July 2010; cited 2011 September 10]; Available from: http://p53.free.fr/Database/p53_cancer_db.html.
10. Van Meir EG, Kikuchi T, Tada M, Li H, Diserens AC, Wojcik BE, et al. Analysis of the p53 gene and its expression in human glioblastoma cells. Cancer Res. 1994 Feb 1; 54(3):649–652. [PubMed: 8306326]

11. Anensen N, Oyan AM, Bourdon JC, Kalland KH, Bruserud O, Gjertsen BT. A distinct p53 protein isoform signature reflects the onset of induction chemotherapy for acute myeloid leukemia. Clin Cancer Res. 2006 Jul 1; 12(13):3985–3992. [PubMed: 16818696]
12. Avery-Kiejda KA, Zhang XD, Adams LJ, Scott RJ, Vojtesek B, Lane DP, et al. Small molecular weight variants of p53 are expressed in human melanoma cells and are induced by the DNA-damaging agent cisplatin. Clin Cancer Res. 2008 Mar 15; 14(6):1659–1668. [PubMed: 18310316]
13. Boldrup L, Bourdon JC, Coates PJ, Sjostrom B, Nylander K. Expression of p53 isoforms in squamous cell carcinoma of the head and neck. Eur J Cancer. 2007 Feb; 43(3):617–623. [PubMed: 17215121]
14. Bourdon JC, Fernandes K, Murray-Zmijewski F, Liu G, Diot A, Xirodimas DP, et al. p53 isoforms can regulate p53 transcriptional activity. Genes Dev. 2005 Sep 15; 19(18):2122–2137. [PubMed: 16131611]
15. Marcel V, Perrier S, Aoubala M, Ageorges S, Groves MJ, Diot A, et al. Delta160p53 is a novel N-terminal p53 isoform encoded by Delta133p53 transcript. FEBS letters. [Research Support, Non-U.S. Gov't]. 2010 Nov 5; 584(21):4463–4468.
16. Ungewitter E, Scrable H. Delta40p53 controls the switch from pluripotency to differentiation by regulating IGF signaling in ESCs. Genes Dev. 2010 Nov 1; 24(21):2408–2419. [PubMed: 21041409]
17. Ghosh A, Stewart D, Matlashewski G. Regulation of human p53 activity and cell localization by alternative splicing. Mol Cell Biol. 2004 Sep; 24(18):7987–7997. [PubMed: 15340061]
18. Courtois S, Verhaegh G, North S, Luciani MG, Lassus P, Hibner U, et al. DeltaNp53, a natural isoform of p53 lacking the first transactivation domain, counteracts growth suppression by wild-type p53. Oncogene. 2002 Oct 3; 21(44):6722–6728. [PubMed: 12360399]
19. Philipova T, Baryawno N, Hartmann W, Pietsch T, Druid H, Johnsen JI, et al. Differential forms of p53 in medulloblastoma primary tumors, cell lines and xenografts. Int J Oncol. 2011 Mar; 38(3): 843–849. [PubMed: 21184030]
20. Khoury MP, Bourdon JC. The isoforms of the p53 protein. Cold Spring Harb Perspect Biol. 2010 Mar.2(3):a000927. [PubMed: 20300206]
21. Mills AA. p53: link to the past, bridge to the future. Genes Dev. 2005 Sep 15; 19(18):2091–2099. [PubMed: 16166374]
22. Rovinski B, Munroe D, Peacock J, Mowat M, Bernstein A, Benchimol S. Deletion of 5'-coding sequences of the cellular p53 gene in mouse erythroleukemia: a novel mechanism of oncogene regulation. Mol Cell Biol. 1987 Feb; 7(2):847–853. [PubMed: 3547084]
23. Yin Y, Stephen CW, Luciani MG, Fahraeus R. p53 Stability and activity is regulated by Mdm2-mediated induction of alternative p53 translation products. Nat Cell Biol. 2002 Jun; 4(6):462–467. [PubMed: 12032546]
24. Ray PS, Grover R, Das S. Two internal ribosome entry sites mediate the translation of p53 isoforms. EMBO Rep. 2006 Apr; 7(4):404–410. [PubMed: 16440000]
25. Grover R, Candeias MM, Fahraeus R, Das S. p53 and little brother p53/47: linking IRES activities with protein functions. Oncogene. 2009 Jul 30; 28(30):2766–2772. [PubMed: 19483723]
26. Matlashewski G, Pim D, Banks L, Crawford L. Alternative splicing of human p53 transcripts. Oncogene Res. 1987 Jun; 1(1):77–85. [PubMed: 2453013]
27. Candeias MM, Powell DJ, Roubalova E, Apcher S, Bourougaa K, Vojtesek B, et al. Expression of p53 and p53/47 are controlled by alternative mechanisms of messenger RNA translation initiation. Oncogene. 2006 Nov 2; 25(52):6936–6947. [PubMed: 16983332]
28. Boldrup L, Bourdon JC, Coates PJ, Sjostrom B, Nylander K. Expression of p53 isoforms in squamous cell carcinoma of the head and neck. Eur J Cancer. [Research Support, Non-U.S. Gov't]. 2007 Feb; 43(3):617–623.
29. Bunz F, Dutriaux A, Lengauer C, Waldman T, Zhou S, Brown JP, et al. Requirement for p53 and p21 to sustain G2 arrest after DNA damage. Science. 1998 Nov 20; 282(5393):1497–1501. [PubMed: 9822382]
30. Kleihues P, Burger PC, Scheithauer BW. The new WHO classification of brain tumours. Brain Pathol. 1993 Jul; 3(3):255–268. [PubMed: 8293185]

31. Singh SK, Hawkins C, Clarke ID, Squire JA, Bayani J, Hide T, et al. Identification of human brain tumour initiating cells. Nature. 2004 Nov 18; 432(7015):396–401. [PubMed: 15549107]
32. Sanai N, Alvarez-Buylla A, Berger MS. Neural stem cells and the origin of gliomas. N Engl J Med. 2005 Aug 25; 353(8):811–822. [PubMed: 16120861]
33. Globus J, Kulenbeck H. Tumors of the striatothalamic and related regions: their probable source of origin and more common forms. Arch Pathol. 1942; 24:674–734.
34. Globus J, Kuhlenbeck H. The subependymal cell plate (matrix) and its relationship to brain tumors of the ependymal type. J Neuropathol Exp Neurol. 1944; 3:1–35.
35. Shoshan Y, Nishiyama A, Chang A, Mork S, Barnett GH, Cowell JK, et al. Expression of oligodendrocyte progenitor cell antigens by gliomas: implications for the histogenesis of brain tumors. Proc Natl Acad Sci U S A. 1999 Aug 31; 96(18):10361–10366. [PubMed: 10468613]
36. Doetsch F, Petreanu L, Caille I, Garcia-Verdugo JM, Alvarez-Buylla A. EGF converts transit-amplifying neurogenic precursors in the adult brain into multipotent stem cells. Neuron. 2002 Dec 19; 36(6):1021–1034. [PubMed: 12495619]
37. Palmer TD, Willhoite AR, Gage FH. Vascular niche for adult hippocampal neurogenesis. J Comp Neurol. 2000 Oct 2; 425(4):479–494. [PubMed: 10975875]
38. Ben-Porath I, Thomson MW, Carey VJ, Ge R, Bell GW, Regev A, et al. An embryonic stem cell-like gene expression signature in poorly differentiated aggressive human tumors. Nat Genet. 2008 May; 40(5):499–507. [PubMed: 18443585]
39. Leonard BW, Mastroeni D, Grover A, Liu Q, Yang K, Gao M, et al. Subventricular zone neural progenitors from rapid brain autopsies of elderly subjects with and without neurodegenerative disease. J Comp Neurol. 2009 Jul 20; 515(3):269–294. [PubMed: 19425077]
40. Medrano S, Burns-Cusato M, Atienza MB, Rahimi D, Scrable H. Regenerative capacity of neural precursors in the adult mammalian brain is under the control of p53. Neurobiol Aging. 2009 Mar; 30(3):483–497. [PubMed: 17850928]
41. Lendahl U, Zimmerman LB, McKay RD. CNS stem cells express a new class of intermediate filament protein. Cell. 1990 Feb 23; 60(4):585–595. [PubMed: 1689217]
42. Doetsch F, Caille I, Lim DA, Garcia-Verdugo JM, Alvarez-Buylla A. Subventricular zone astrocytes are neural stem cells in the adult mammalian brain. Cell. 1999 Jun 11; 97(6):703–716. [PubMed: 10380923]
43. Laywell ED, Kukekov VG, Steindler DA. Multipotent neurospheres can be derived from forebrain subependymal zone and spinal cord of adult mice after protracted postmortem intervals. Exp Neurol. 1999 Apr; 156(2):430–433. [PubMed: 10328947]
44. Imura T, Kornblum HI, Sofroniew MV. The predominant neural stem cell isolated from postnatal and adult forebrain but not early embryonic forebrain expresses GFAP. J Neurosci. 2003 Apr 1; 23(7):2824–2832. [PubMed: 12684469]
45. Imura T, Nakano I, Kornblum HI, Sofroniew MV. Phenotypic and functional heterogeneity of GFAP-expressing cells in vitro: differential expression of LeX/CD15 by GFAP-expressing multipotent neural stem cells and non-neurogenic astrocytes. Glia. 2006 Feb; 53(3):277–293. [PubMed: 16267834]
46. Garcia AD, Doan NB, Imura T, Bush TG, Sofroniew MV. GFAP-expressing progenitors are the principal source of constitutive neurogenesis in adult mouse forebrain. Nat Neurosci. 2004 Nov; 7(11):1233–1241. [PubMed: 15494728]
47. Doetsch F, Garcia-Verdugo JM, Alvarez-Buylla A. Cellular composition and three-dimensional organization of the subventricular germinal zone in the adult mammalian brain. J Neurosci. 1997 Jul 1; 17(13):5046–5061. [PubMed: 9185542]
48. Reynolds BA, Tetzlaff W, Weiss S. A multipotent EGF-responsive striatal embryonic progenitor cell produces neurons and astrocytes. J Neurosci. 1992 Nov; 12(11):4565–4574. [PubMed: 1432110]
49. Reynolds BA, Weiss S. Generation of neurons and astrocytes from isolated cells of the adult mammalian central nervous system. Science. 1992 Mar 27; 255(5052):1707–1710. [PubMed: 1553558]

50. Reynolds BA, Weiss S. Clonal and population analyses demonstrate that an EGF-responsive mammalian embryonic CNS precursor is a stem cell. Dev Biol. 1996 Apr 10; 175(1):1–13. [PubMed: 8608856]
51. Gard AL, Pfeiffer SE. Two proliferative stages of the oligodendrocyte lineage (A2B5+O4- and O4+Galc-) under different mitogenic control. Neuron. 1990 Nov; 5(5):615–625. [PubMed: 2223090]
52. Buffo A, Rite I, Tripathi P, Lepier A, Colak D, Horn AP, et al. Origin and progeny of reactive gliosis: A source of multipotent cells in the injured brain. Proc Natl Acad Sci U S A. 2008 Mar 4; 105(9):3581–3586. [PubMed: 18299565]
53. Lang B, Liu HL, Liu R, Feng GD, Jiao XY, Ju G. Astrocytes in injured adult rat spinal cord may acquire the potential of neural stem cells. Neuroscience. 2004; 128(4):775–783. [PubMed: 15464285]
54. Petitjean A, Achatz MI, Borresen-Dale AL, Hainaut P, Olivier M. TP53 mutations in human cancers: functional selection and impact on cancer prognosis and outcomes. Oncogene. 2007 Apr 2; 26(15):2157–2165. [PubMed: 17401424]
55. Oren M, Rotter V. Mutant p53 gain-of-function in cancer. Cold Spring Harb Perspect Biol. 2010 Feb.2(2):a001107. [PubMed: 20182618]
56. Goh AM, Coffill CR, Lane DP. The role of mutant p53 in human cancer. J Pathol. 2011 Jan; 223(2):116–126. [PubMed: 21125670]
57. Sasaki T, Maier B, Bartke A, Scrable H. Progressive loss of SIRT1 with cell cycle withdrawal. Aging Cell. 2006 Oct; 5(5):413–422. [PubMed: 16939484]
58. Carlson BL, Pokorny JL, Schroeder MA, Sarkaria JN. Establishment, Maintenance and in vitro and in vivo Applications of Primary Human Glioblastoma Multiforme (GBM) Xenograft Models for Translational Biology Studies and Drug Discovery. Curr Protoc Pharmacol. 2011 Mar; 52(14):1–14.
59. Murray-Zmijewski F, Lane DP, Bourdon JC. p53/p63/p73 isoforms: an orchestra of isoforms to harmonise cell differentiation and response to stress. Cell Death Differ. 2006 Jun; 13(6):962–972. [PubMed: 16601753]
60. Ishii N, Maier D, Merlo A, Tada M, Sawamura Y, Diserens AC, et al. Frequent co-alterations of TP53, p16/CDKN2A, p14ARF, PTEN tumor suppressor genes in human glioma cell lines. Brain Pathol. 1999 Jul; 9(3):469–479. [PubMed: 10416987]
61. Gritti, A.; Galli, R.; Vescovi, A. Protocols for Neural Cell Culture. 3rd ed.. Fedoroff, S.; Richardson, A., editors. Totowa: Humana Press, Inc; 2001.

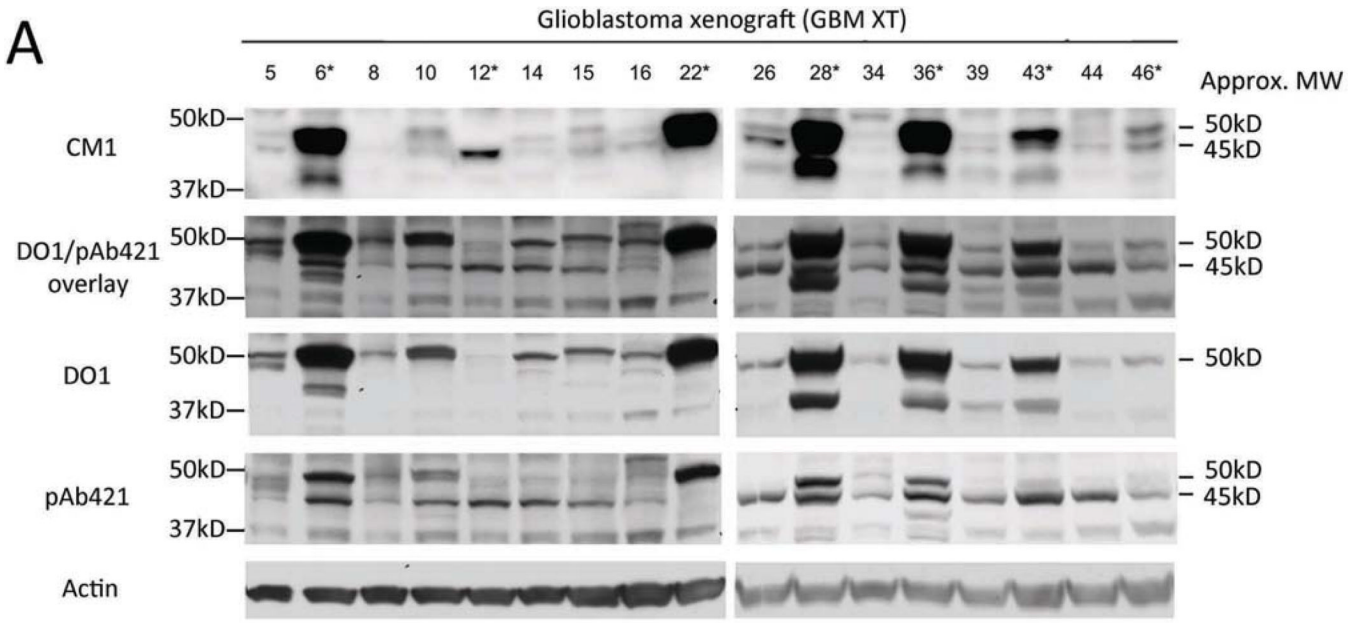

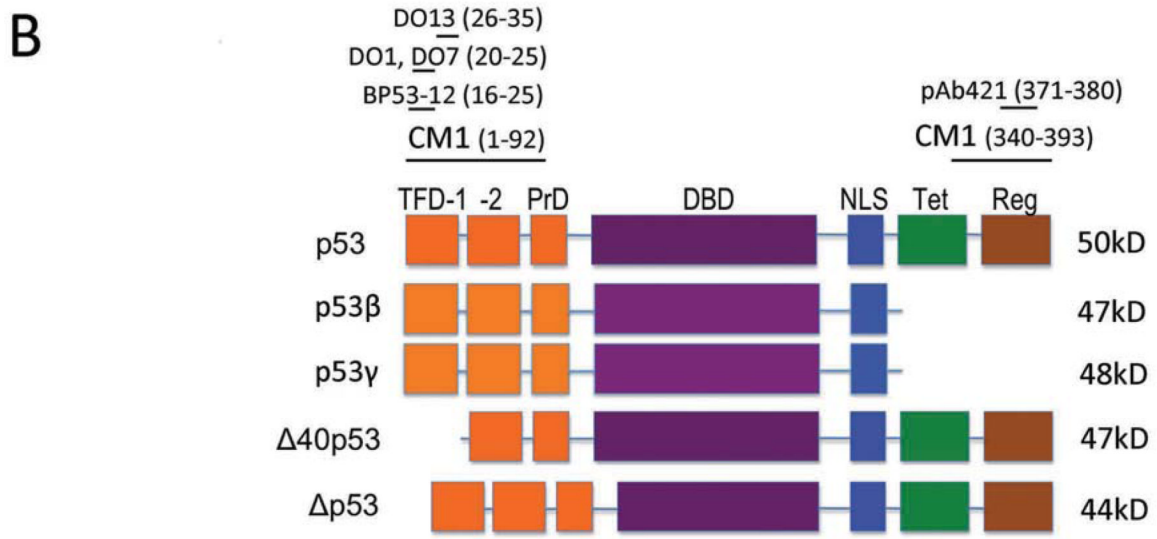

Figure 1. Δ40p53 is a major isoform in glioblastoma

(A) Western blot analysis of p53 isoforms in glioblastoma xenograft (GBM XT) samples using CM1, DO1, and pAb421. Approximate molecular weights (Approx. MW) are given to the right, indicating p53 (50kD) and a smaller isoform (45kD) that is detected by pAb421 and not DO1. The DO1/pAb421 overlay shows that the 45kD band is distinct from another band detected by DO1 that ran closer to the 37kD marker (most prominent in GBM XT 28 and 36). Single asterisk (*) indicates samples with a p53 DNA binding domain mutation (see Table I). **(B)** Diagrammatic representation of the p53 isoforms identified in this study. p53 domains are indicated by boxes: transcription factor domain (TFD-1, -2), proline domain (PrD), DNA binding domain (DBD), nuclear localization signal (NLS), tetramerization domain (Tet), regulatory (basic) domain (Reg). Antibodies used to recognize specific isoforms are indicated at the top. DO1, DO7, and BP53-12 recognize N-terminal epitopes of

p53 and pAb421 recognizes the C-terminus (will not detect β or γ isoforms). The pAb421 epitope overlaps with several post-translational modifications. CM1 is a rabbit polyclonal antibody raised against full-length p53.

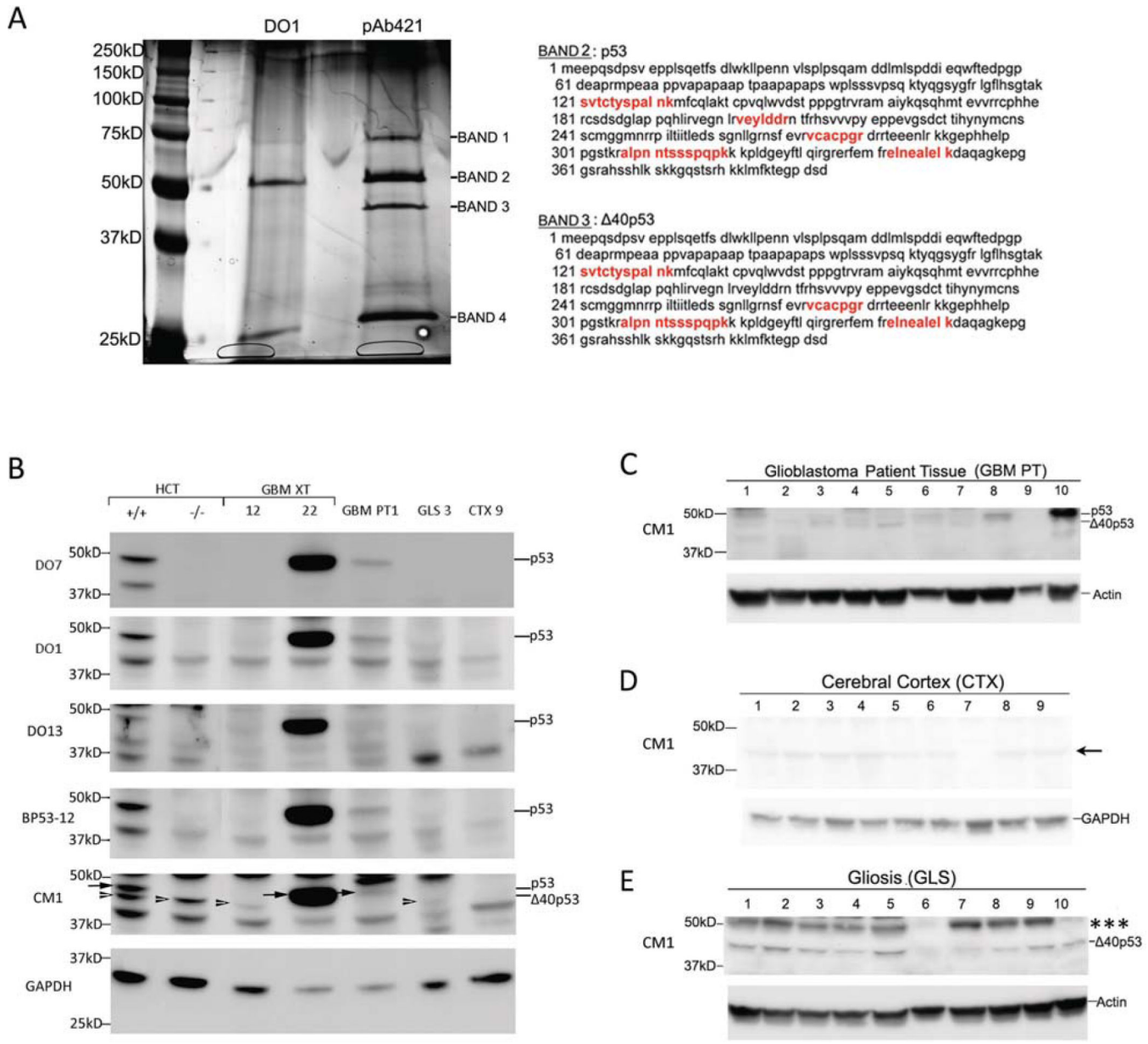

Figure 2. Identification of p53 and Δ40p53 by mass spectrometry and isoform expression in patient glioblastoma, cortex, and gliosis

(A) Mass spectrometric identification of p53 and Δ40p53. p53 protein was immunoprecipitated from GBM XT 43 using either DO1 or pAb421. Immunoprecipitates were subjected to SDS-PAGE and the gel was silver stained. Bands 1, 2, and 3 were submitted for mass spectrometric analysis. Peptide sequences in bands 2 and 3 that matched human p53 are indicated in red. No human p53 peptide sequences were recovered from bands 1 or 4. Of the recovered peptide sequences, vcacpgr, alpnntssspqpk and elnealelk are found in Δ40p53 but missing in Δp53 and p53β/y, respectively. Based on the known isoforms that migrate at approximately 45kD (p53β/γ, Δ40p53, and Δp53), the mass spectrometry data indicate that the 45kD band is Δ40p53. **(B)** p53 isoform detection in representative glioblastoma xenografts, primary tissue, gliosis and cortex. Extracts of HCT116 cells with intact p53 (HCT+/+) and HCT116 cells with an insertion of Neo^R into

exon 2 (HCT−/−) are used as a reference for p53 (arrow) and Δ40p53 (arrowhead), respectively. Isoforms were detected on western blots using a panel of antibodies: a polyclonal antibody, CM1, or N-terminal monoclonal antibodies (D07, D01, and BP53-12). GBM XT 12 expresses only the 45kD band (arrowhead) and GBM XT 22 expresses the upper 50kD band (arrowhead). The 45kD band in GLS 3 co-migrates with the Δ40p53 band in HCT cells (see arrowheads). **(C)** Western blot analysis of 10 glioblastoma patient (GBM PT) frozen tissue samples using CM1. Δ40p53 and p53 were detected at lower levels than in GBM XT samples with the exception of GBM PT 10 where p53 level was comparable to GBM XT with DNA binding domain mutations (Fig. 1A). **(D)** Nine cerebral cortex (CTX) and **(E)** ten gliosis (GLS) tissues were analyzed for p53 isoform expression using CM1. We detected a 45kD band in gliosis samples that co-migrated with the Δ40p53 band in HCT cells (B, arrowheads). Gliosis samples showed an isoform that migrated with an apparent MW of ~55kD indicated by *** (see Fig. S2 and S3). Arrow next to CTX samples (D) indicates a band that was found in p53-null cells (Supplement Fig. S4). This band migrated below the Δ40p53 band when aligned with other samples including HCT cells, GBM XT 12, and GLS 3 (B). Western blot images were cropped for clarity and focus on relevant bands.

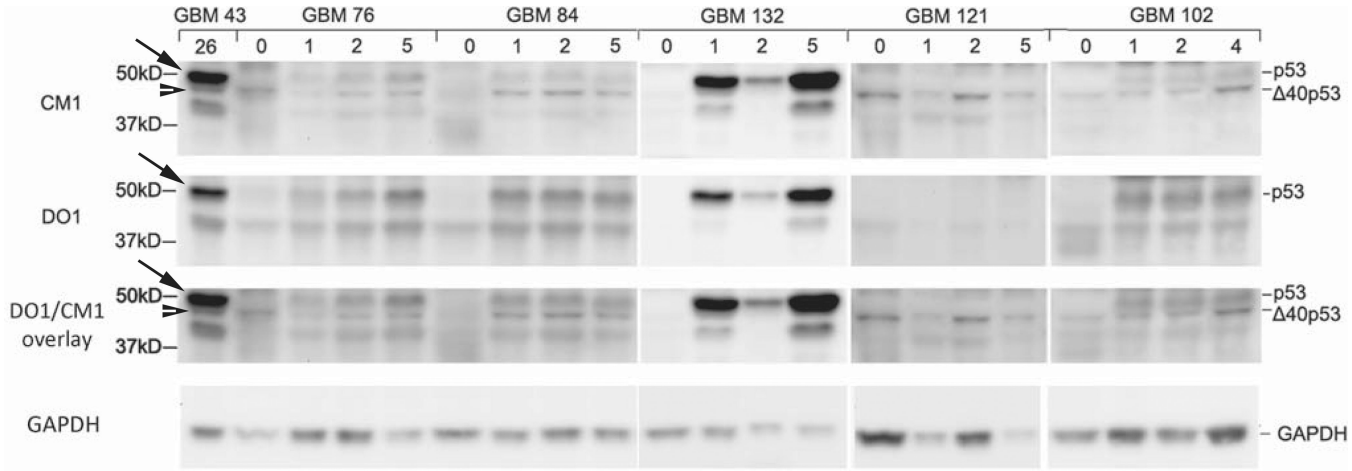

Figure 3. Full-length p53 is associated with the tumor component of glioblastoma patient tissue

Western blot analysis of GBM PT (passage zero) and corresponding GBM XT (passage 1, 2, 4, or 5) using CM1 (top panel) and DO1 (middle panel). GBM XT 43 (passage 26) was used as a control to align p53 (arrow) and Δ40p53 (arrowhead) at ~50 and 48 kD, respectively. The 48kD band was detected by CM1 (not DO1) and corresponds to the 48kD band initially detected by pAb421 (Fig. 1A). DO1 does not recognize mouse p53 species. A DO1/CM1 overlay is included for clarity and western blot images were cropped to focus on relevant bands.

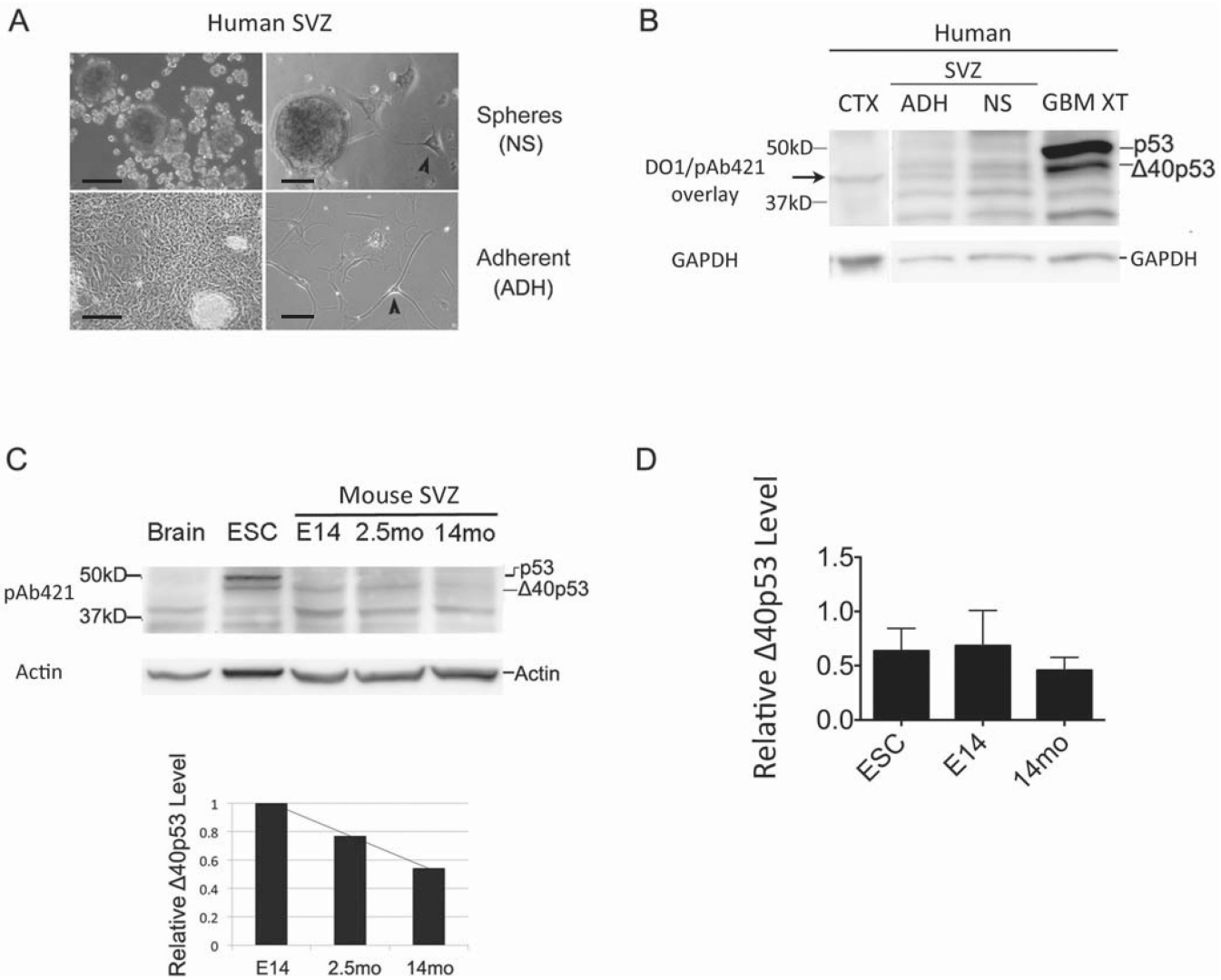

Figure 4. Δ40p53 is expressed in subventricular zone (SVZ) progenitor cells of the brain and decreases with age

(A) Adult neural progenitor cells were derived from the subventricular zone (SVZ) of elderly subjects post-mortem and grown in culture as neurospheres (NS) or as an adherent (ADH) monolayer. Scale bars indicate 10μm. Arrowheads indicate cells with long processes (>4 times length of cell body) that morphologically resembled neurons. **(B)** p53 isoform expression analysis in adult human SVZ cells compared to glioblastoma xenograft (GBM XT) and cerebral cortex (CTX) by western blot analysis using DO1 and pAb421 (overlay shown). GBM XT is shown as a positive control for Δ40p53 expression and CTX as a negative control. Arrow indicates a band that migrated below Δ40p53 and co-migrated with a band found in p53-null cells (see Fig. S4). **(C)** SVZ-derived neural progenitor cells from embryonic day 14 (E14) or adult brain at 2.5 months (2.5mo) and 14 months (14mo) of age analyzed by western blot using pAb421. p53 isoform expression was compared to total brain tissue (expresses neither p53 or Δ40p53) and mouse embryonic stem cells (ESC), which expresses both. Bar graph below shows relative Δ40p53 levels from the western blot above, and triplicate experiments are represented in **(D)**. Analysis of variance (ANOVA) did not reveal statistically significant differences between groups despite the decreasing trend in

Δ40p53 levels observed in SVZ cultures from older mice (see main text). Western blot images were cropped to enhance clarity and focus on relevant p53 bands.

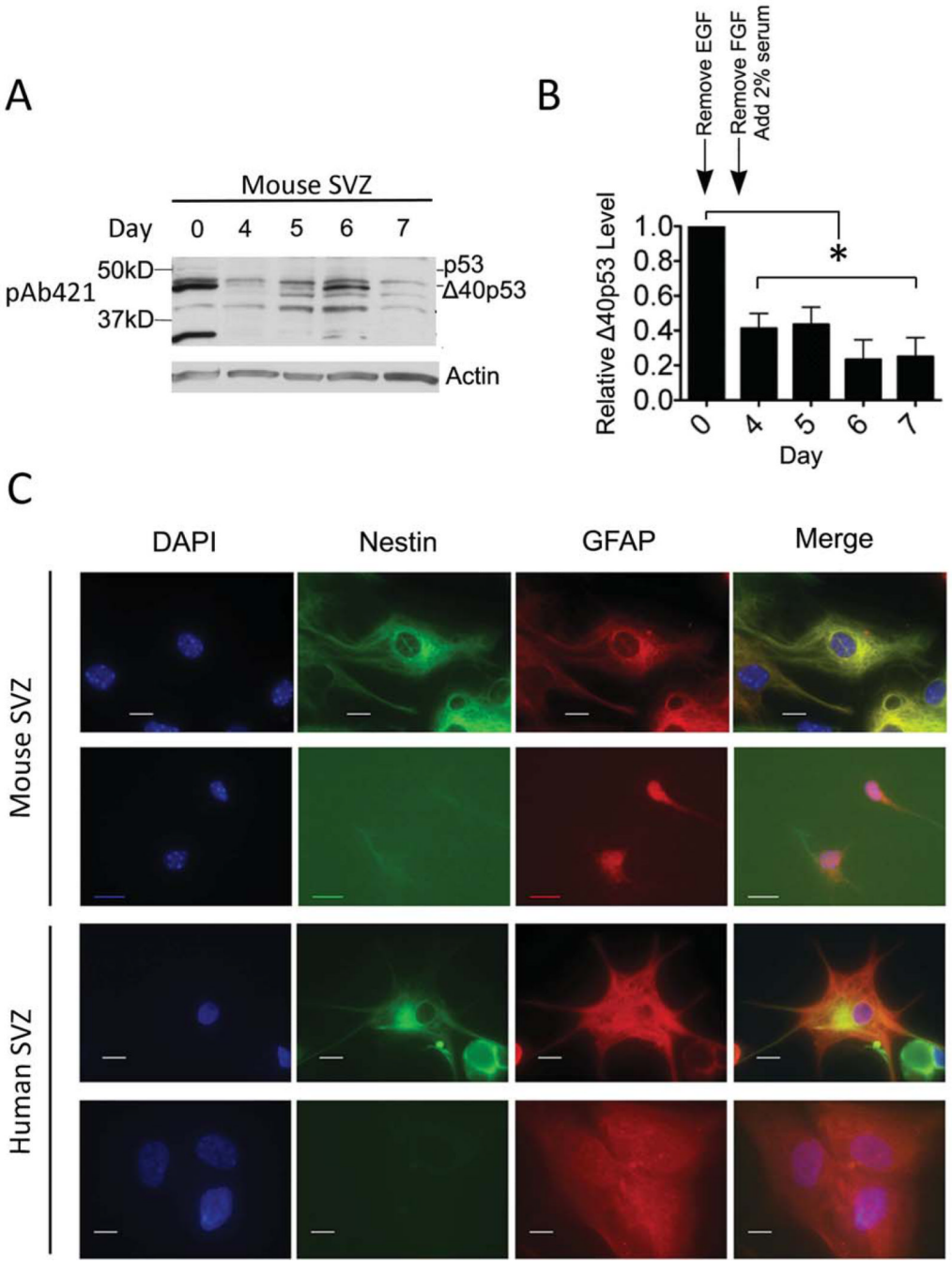

Figure 5. Differentiation decreases Δ40p53 in subventricular (SVZ) progenitor cells

(A) Mouse SVZ-derived cells subjected to *in vitro* differentiation for 7 days. SVZ cells previously maintained in medium containing growth factors, fibroblast growth factor (FGF) and epidermal growth factor (EGF), were plated on poly-(L)-ornithine-treated tissue culture plates without EGF on day 0. On day 3, FGF was also removed and 2% fetal bovine serum was added to the culture medium. Cells were collected at approximately the same time each day for a total of 7 days and analyzed by western blot using pAb421. **(B)** Quantification of Δ40p53 protein levels relative to day 0. Analysis of variance (ANOVA) revealed a significant decrease in relative Δ40p53 levels in days 4 through 7 compared to day 0.

Changes in culture media are indicated above the bar graph. **(C)** Immunofluorescence analysis of differentiated mouse (top panels) and adult human SVZ cells (bottom panels). Cells were stained with differentiation markers, nestin and GFAP, and counterstained with DAPI to identify nuclei. Scale bar represents 10μM. Western blot image was cropped to enhance clarity and focus on p53 species

Oncogene. Author manuscript; available in PMC 2014 January 28.

Table I

Clinicopathological characteristics and p53 mutation status of xenograft tumors (GBM XT).

GBM XT	Diagnosis	Gender Male (M), Female (F)	Age at resection	Location	p53 mutation
5	GBM	M	57	Right temporal	None
6	GBM	M	65	Left frontal	273: Arg>Cys
8	GBM	F	75	Right parietal	None
10	Grade 4 oligoastrocytoma	M	41	Right temporal	None
12	GBM	M	68	Right parietal	Ex5: GT>CT 5' splice site*
14	GBM	M	58	Right temporal	None
15	GBM	Information not available			None
16	GBM	Information not available			None
22	Grade 4 gliosarcoma	M	80	Frontal temporal	273: Arg>Cys
26	GBM	M	48	Right frontal	None
28	Grade 4 gliosarcoma	M	67	Left temporoparietal	246: Met>Thr
34	GBM	F	46	Left occipital	None
36	GBM	M	53	Left cerebellum	132: Lys>Met
39	GBM	M	52	Left frontal	None
43	GBM	M	69	Right temporal	270: Phe>Cys
44	GBM	F	79	Left frontal	None
46	GBM	M	55	Right parietal	N/A

*Genomic sequencing identified a GT to CT transversion in the donor splice site for intron 5. cDNA sequencing indicated that this resulted in utilization of a cryptic splice donor site 43bp upstream of the normal donor site, which caused deletion of 14 amino acids at the 3' end of exon 5. Exon 6 sequences were present in their entirety. The resultant Δ40p53 protein is missing a short piece of the DNA binding domain.

Table II

Clinicopathological features of patient tumors (GBM PT).

GBM PT	Diagnosis	Gender Male (M), Female (F)	Age at resection	Location	% Tumor cells
1	GBM	M	47	Parietal occipital	>80%
2	GBM	F	44	Left frontal	75%
3	GBM	M	71	Right temporal	>80%
4	GBM	M	56	Right temporal	50%
5	GBM	M	23	Right parietal	60%
6	GBM	F	71	Left frontal	>80%
7	GBM	M	46	Left temporal	>80%
8	GBM (secondary)	M	51	Right temporal	70–80%
9	GBM	F	78	Right frontal	60%
10	GBM	M	73	Parietooccipital	>80%

Table III

Distribution of stem and progenitor cells in human and mouse NSC cultures based on indicated ICC markers.

	Nestin and GFAP	Nestin	GFAP	β-tubulin	O4
Mouse NSC (Day 7)	19/100 (19%)	None	89/100 (89%)	None	None
Human NSC	44/121 (36%)	None	42/109 (39%)	None	13/117 (11%)